Non return to zero line coding with suppressed carrier in FSO transceiver systems under light rain conditions

Article *in* Journal of Optical Communications · July 2022

DOI: 10.1515/joc-2022-0039

Ahmed Nabih Zaki Rashed*, Malek G. Daher, S. K. Hasane Ahammad, Francis Jesmar P. Montalbo, Vishal Sorathiya, Sayed Asaduzzaman, Hasin Rehana and Asif Zuhayer

Non return to zero line coding with suppressed carrier in FSO transceiver systems under light rain conditions

https://doi.org/10.1515/joc-2022-0039
Received March 10, 2022; accepted June 23, 2022;
published online July 13, 2022

Abstract: This paper aims to simulate performance efficiency of carrier suppressed non return to zero line coding based FSO transceiver systems under light rain conditions with amplification units at 40 Gbps. The max. *Q*, BER and total optical power are simulated and demonstrated after FSO channel and PIN Photodetector Receiver under light rain weather conditions at maximum reach of 1.2 km at 10 Gbps. As well as the max. *Q* Factor variations versus max reach variations are clarified after PIN photodetector receiver under light rain weather conditions at 10, 40 Gbps with/without amplification units. Besides the total optical power variations versus max reach variations are assured after FSO channel under light rain weather conditions at 10, 40 Gbps with/without amplification units.

Keywords: amplification units; carrier suppressed; light rain; NRZ line coding.

***Corresponding author: Ahmed Nabih Zaki Rashed**, Electronics and Electrical Communications Engineering Department, Faculty of Electronic Engineering, Menoufia University, Menouf, 32951, Egypt, E-mail: ahmed_733@yahoo.com. https://orcid.org/0000-0002-5338-1623
Malek G. Daher, Physics Department, Islamic University of Gaza, P.O. Box 108, Gaza, Palestine, Egypt; and School of Physics, Universiti Sains Malaysia, 11800, Penang, Malaysia, E-mail: malekjbreel20132017@gmail.com
S. K. Hasane Ahammad, Department of ECE, Koneru Lakshmaiah Education Foundation, 522302, Vaddeswaram, Andhra Pradesh, India, E-mail: ahammadklu@gmail.com
Francis Jesmar P. Montalbo, College of Informatics and Computing Sciences, Batangas State University, Batangas, 4200, Philippines, E-mail: francismontalbo@ieee.org
Vishal Sorathiya, Faculty of Engineering and Technology, Parul Institute of Engineering and Technology, Parul University, Waghodia Road 391760, Vadodara, Gujarat, India, E-mail: vishal.sorathiya9@gmail.com
Sayed Asaduzzaman and Hasin Rehana, Department of Computer Science and Engineering, Rangamati Science and Technology University, Rangamati, Bangladesh; and Department of Computer Science and Engineering, Daffodil International University, Dhaka, Bangladesh, E-mail: asadcse.rmstu@gmail.com (S. Asaduzzaman), hasin.cse13@gmail.com (H. Rehana)
Asif Zuhayer, Department of Electronics & Telecommunication Engineering, Chittagong University of Engineering and Technology, Chattogram, 4349, Bangladesh, E-mail: u1608018@student.cuet.ac.bd

1 Introduction

The free space optics communication systems represents new trend in various current applications which based on optical media as well as air media to have improvement of transmission characteristics like high transmission security high speed accessing in addition to shrinking the system cost [1–18]. Furthermore the most important specification of free space optics communication system is the establishment of this communication without spectrum license requirements, in addition to their transmission has no electromagnetic interference [19–37]. However the drawback of free space optics transmission through the atmosphere layer of air media circumstance has directly effectiveness on transmission characteristics of free space optical link but also the surrounding environment. However the dominant challenge of free space optical link is the attenuation [38–56]. Hence the weather conditions play an important role in degradation of system performance and increasing attenuation. There are many essential resources causes attenuation like snows, fogs and rains [57–73]. Free space optical transmission extended for large distances at high power levels in addition to low power utilization [74–89]. Other challenges face the free space optics is aerosol scattering generated from rains, fogs and snows. In addition to free space optic links exposed to atmospheric turbulence resulting scintillation [90–118].

This work has been simulated the performance efficiency of carrier suppressed non return to zero line coding based FSO transceiver systems under light rain conditions with amplification units at 40 Gbps. We have studied the max. *Q* Factor variations versus max reach variations are clarified after the photodetector under light rain weather conditions at 10, 40 Gbps with/without amplification units. Also we have studied the total optical power variations versus max reach variations are assured after FSO channel under light rain weather conditions at 10, 40 Gbps with/without amplification units. The max. Q, BER and total optical power are simulated and demonstrated after FSO channel and PIN Photodetector Receiver under light rain weather conditions at maximum reach of 1.2 km at 10 Gbps.

2 Simulation setup

Figures 1 and 2 show the simplified block diagram of FSO transceiver system and FSO transceiver simulation model description. The input electrical signal is modulated through the electro optic modulators. The source converts the signal to the optical signal. The free space medium has two lenses to concentrate the light to be in high intensity. The light signal is modulated through the free space optics medium. The light detector detects the electrical signal. The electrical form is demodulated with the demodulator to get the output electrical form.

The data source generator generates stream bits sequence within the line coding of return to zero code. Fork unit distribute the signals into directions. First direction to electrical gain and second direction to LiNb Mach–Zehnder modulator. On the other hand, the electrical bit coded signal is modulated through laser measured which transforms from the light signal to optical signal form. The two electrical signals and the light carrier signal are injected together through electro optic modulators (LiNb Mach–Zehnder modulator). The sine generators generate the electrical signal with a frequency of 100 GHz and phase shift of −10°. The generated signal is directed to the fork unit.

The fork unit distributes the signals to the electrical gain and electro optic modulators (LiNb MZM). The modulated signal is forward to the amplification units. Amplifiers are used to reduce the attenuation and compensate the losses in the FSO channel. The free space optics channel has light rain with signal attenuation of 10 dB/km. The light signal is passed to PIN photodetector in order to be converted to the electrical. The signal is filtered from the ripples with LPBFs. The signal is reshaped, retimed and regeneration through 3R regenerator. Q

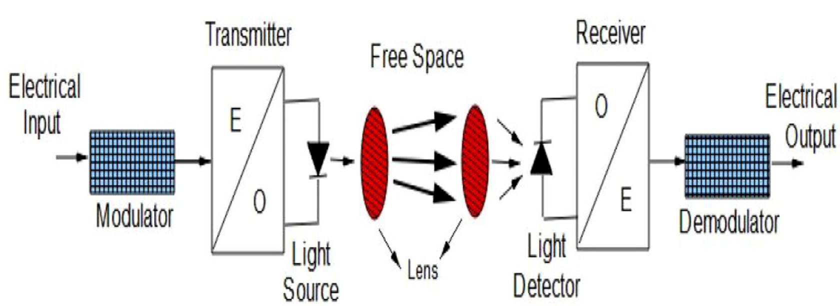

Figure 1: Simplified block diagram of FSO transceiver system.

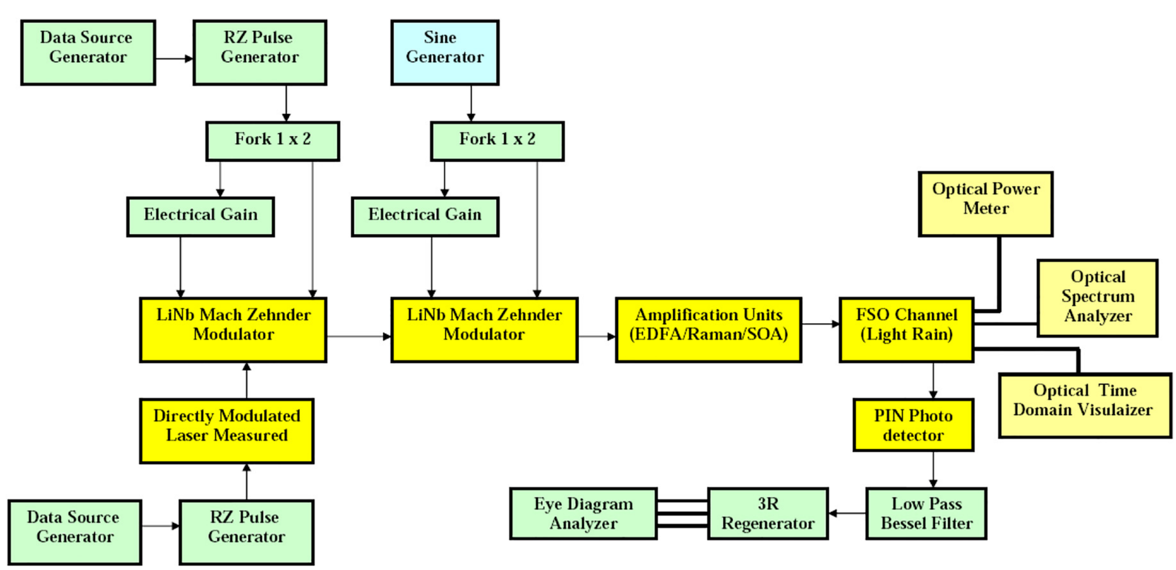

Figure 2: FSO transceiver simulation model description.

value and min BER values are tested with eye analyzers. The optical signal intensity levels with spectral time and frequency variations through FSO channel are measured by using optical time domain visualizers/optical spectrum analyzer/optical power meter under light rain weather conditions.

3 Results with discussions

We have been simulated max. Q and min. BER after PIN photodetector receiver under light rain weather conditions at maximum reach of 1.2 km at 10, 40 Gbps. The total optical power is simulated also after FSO channel under light rain weather conditions at maximum reach of 1.2 km at 10, 40 Gbps. The max signal power level is clarified versus time duration and spectral wavelength after FSO channel under light rain weather conditions at maximum reach of 1.2 km at 10, 40 Gbps. The max. Q factor variations versus max reach variations are demonstrated after PIN photodetector receiver under light rain weather conditions at 10, 40 Gbps with/without amplification units. Moreover the total optical power variations versus max reach variations are demonstrated after FSO channel under light rain weather conditions at 10, 40 Gbps with/without amplification units. The results are clarified depends upon the parameter in Table 1.

Table 1: Variables for the proposed article.

Parameters	**Values/units**
Optical transmitter	
Laser frequency	1550 nm
Laser power	20 mW
Threshold current	20 mA
Maximum current	300 mA
FSO channel	
Attenuation (light rain)	10 dB/km [1]
Reach	1.2–6 km
Tx./Rx. aperture diameter	5, 30 cm
Beam divergence	1 mrad
Tx./Rx. loss	0 dB
PIN photodetector	
Gain	3
Insertion loss	0 dB

Figure 3 shows max. Q and min. BER after PIN photodetector receiver under light rain weather conditions at maximum reach of 1.2 km at 10 Gbps without amplification unit. Where max Q factor, min BER are 9.31, 5.76×10^{-21}, respectively.

Figure 4 demonstrates max. Q and min. BER after PIN photodetector receiver under light rain weather conditions at maximum reach of 1.2 km at 40 Gbps without amplification unit. Where max Q Factor, min BER are 5.88, 1.95×10^{-9}, respectively. The study emphasized that the higher the data rate can be achieved the lower Q factor can be measured.

Figure 5 shows the total optical power after FSO channel under light rain weather conditions at maximum reach of 1.2 km at 10 Gbps without amplification unit. The total optical power is 2.457 µW in this case.

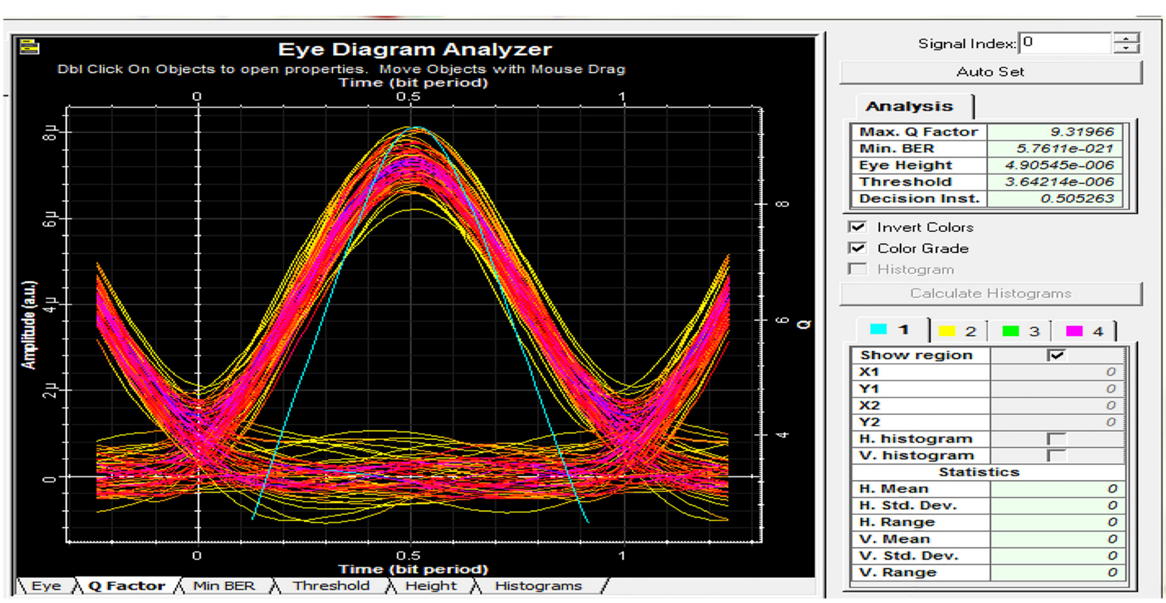

Figure 3: Max. Q and min. BER after PIN photodetector under light rain weather conditions at 1.2 km at 10 Gbps.

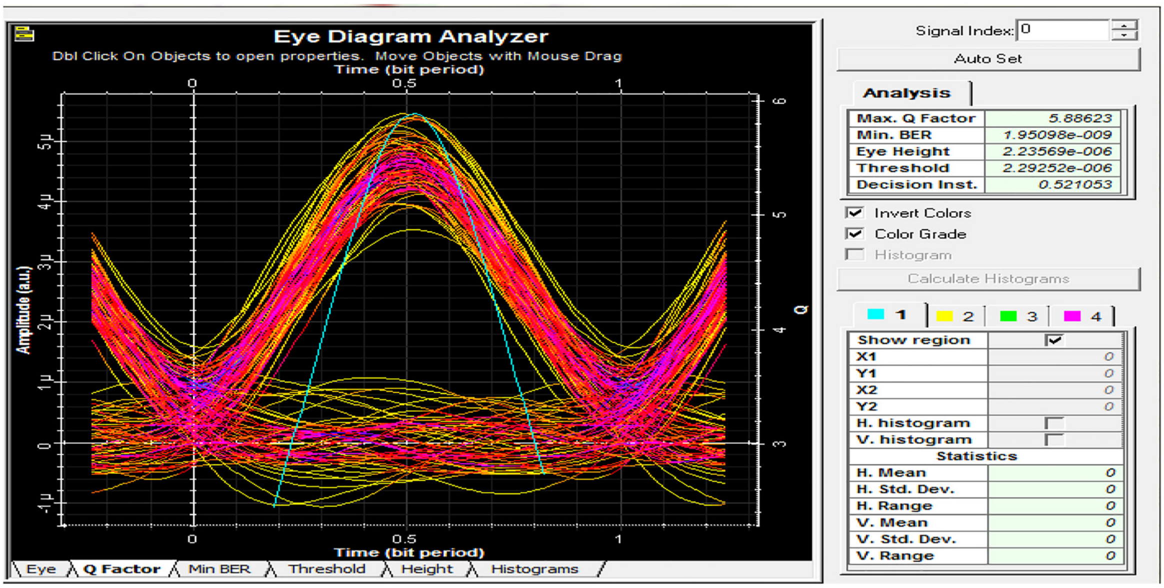

Figure 4: Max. Q and min. BER after PIN photodetector under light rain weather conditions at 1.2 km at 40 Gbps.

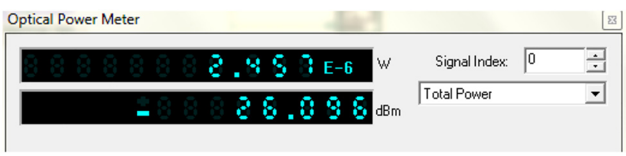

Figure 5: Total optical power after FSO channel under light rain weather conditions at maximum reach of 1.2 km at 10 Gbps.

Figure 6 clarifies the total optical power after FSO channel under light rain weather conditions at maximum reach of 1.2 km at 40 Gbps without amplification unit. The total optical power is 1.552 μW in this case.

Figure 7 demonstrates the max power with time duration after FSO channel under light rain weather conditions at maximum reach of 1.2 km at 10 Gbps without amplification unit. Where the max signal power (MSP), noise power (NP) are 21.044 μW, –1.002 μW, respectively.

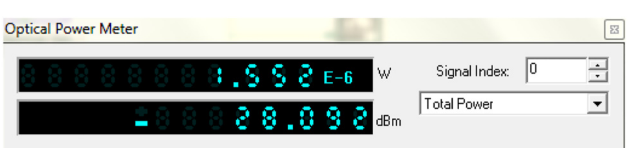

Figure 6: Total optical power after FSO channel under light rain weather conditions at maximum reach of 1.2 km at 40 Gbps.

Figure 8 assures the max power versus time duration after FSO channel under light rain weather conditions at maximum reach of 1.2 km at 40 Gbps without amplification unit. Where MSP, NP are 13.29 μW, –0.6329 μW, respectively.

Figure 9 illustrates the max signal power level versus spectral wavelength after FSO channel under light rain weather conditions at maximum reach of 1.2 km at 10 Gbps. Where the MSP, NP are –32.6119 dBm, –103.209 dBm respectively.

Figure 10 clarifies the max signal power level versus spectral wavelength after FSO channel under light rain weather conditions at maximum reach of 1.2 km at 40 Gbps. Where MSP, NP are –34.7075 dBm, –103.109 dBm respectively.

Figure 11 clarifies the max. Q Factor variations versus max reach variations after PIN Photodetector Receiver under light rain weather conditions at 10 Gbps with/without amplification units. The max Q factor is 17.65 with the amplification unit, 9.31 without the amplification unit at reach of 1.2 km. As well as the max Q is 15 with the amplification unit, 7.54 without the amplification unit at reach of 2.4 km. Also the max Q is 12 with the amplification unit, 5.32 without the amplification unit at reach of 3.6 km. Besides the max Q is 10 with the amplification unit, 3.65 without the amplification unit at reach of 4.8 km. Moreover the max Q is 9 with the amplification unit, 2.54 without the amplification unit at reach of 6 km.

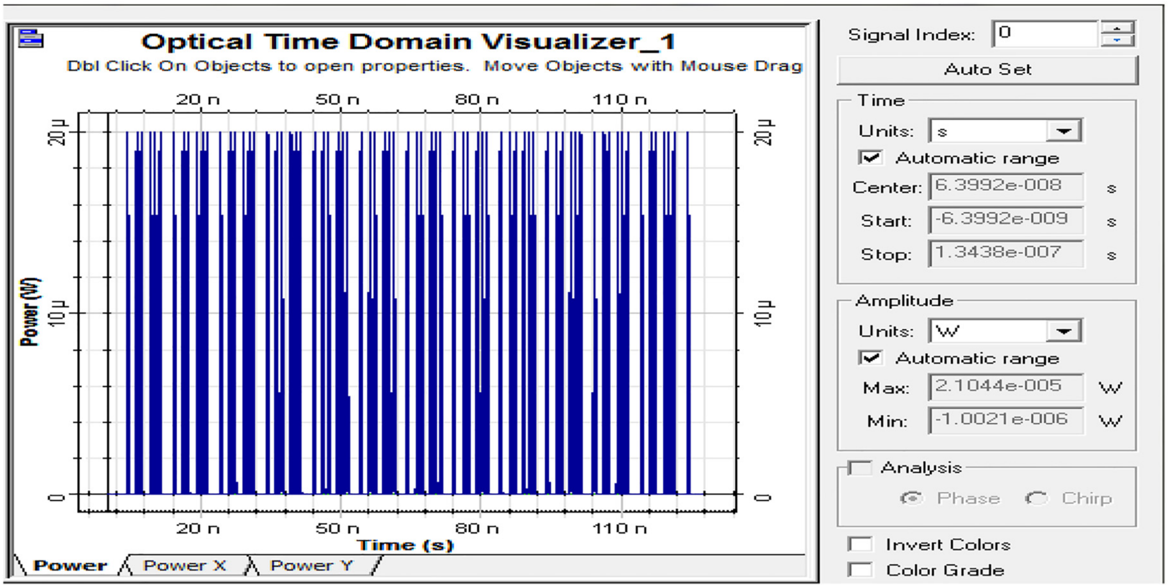

Figure 7: Max signal power level versus time duration after FSO channel under light rain weather conditions at maximum reach of 1.2 km at 10 Gbps.

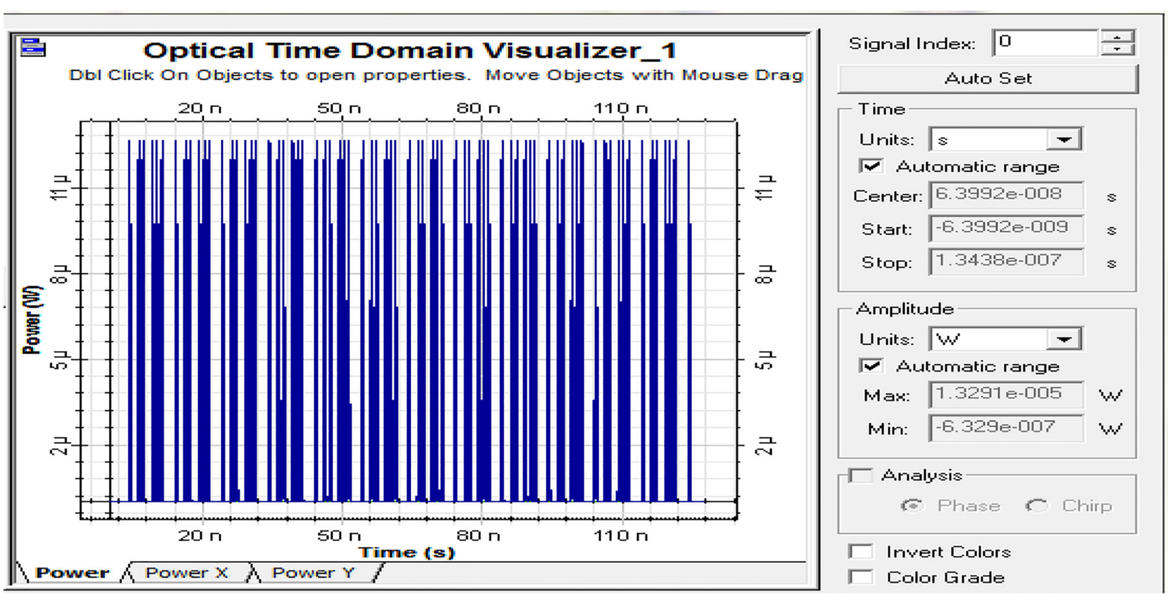

Figure 8: Max signal power level versus time duration after FSO channel under light rain weather conditions at maximum reach of 1.2 km at 40 Gbps.

Figure 12 clarifies the max. *Q* variations versus max reach variations after PIN photodetector receiver under light rain weather conditions at 40 Gbps with/without amplification units. The max *Q* is 12 with the amplification unit, 5.32 without the amplification unit at reach of 1.2 km. As well as the max *Q* is 10 with the amplification unit, 3.65 without the amplification unit at reach of 2.4 km. Also the max *Q* is 9 with the amplification unit, 2.54 without the amplification unit at reach of 3.6 km. Besides the max *Q* is 6 with the amplification unit, 1.8 without the amplification unit at reach of 4.8 km. Moreover the max *Q* is 3.87 with the amplification unit, 1.21 without the amplification unit at reach of 6 km. The study assured that the max *Q* is degraded with the FSO channel reach increases.

Figure 13 demonstrates the total optical power variations versus max reach variations after FSO channel under

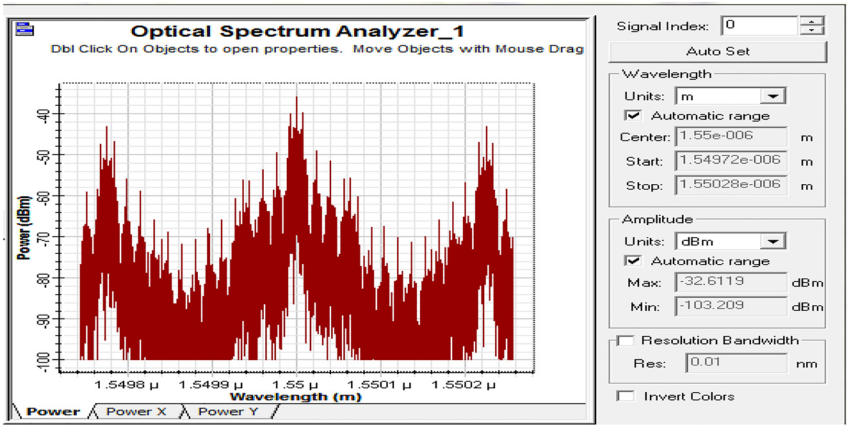

Figure 9: Max signal power level versus spectral wavelength after FSO channel under light rain weather conditions at maximum reach of 1.2 km at 10 Gbps.

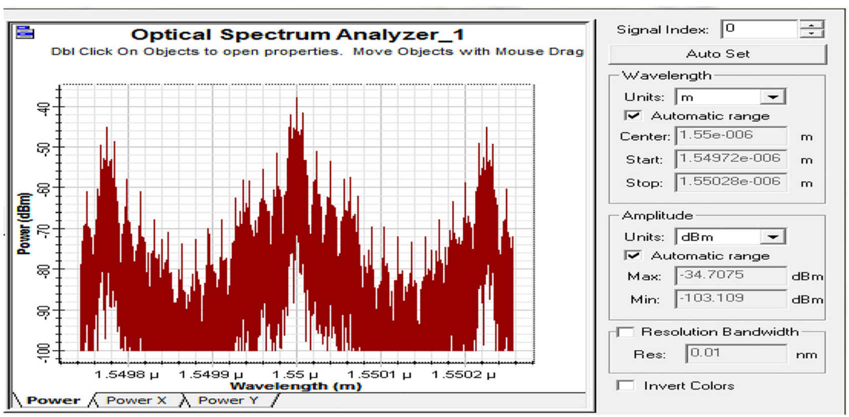

Figure 10: Max signal power level versus spectral wavelength after FSO channel under light rain weather conditions at maximum reach of 1.2 km at 40 Gbps.

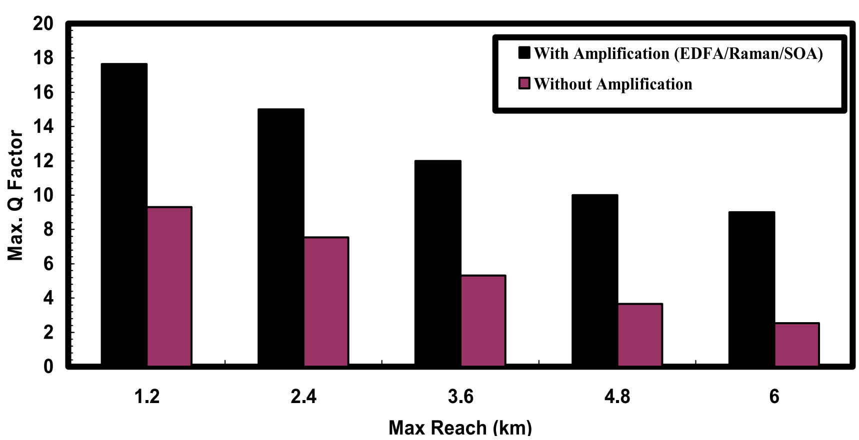

Figure 11: Max. *Q* factor variations versus max reach variations after PIN photodetector receiver under light rain weather conditions at 10 Gbps with/ without amplification units.

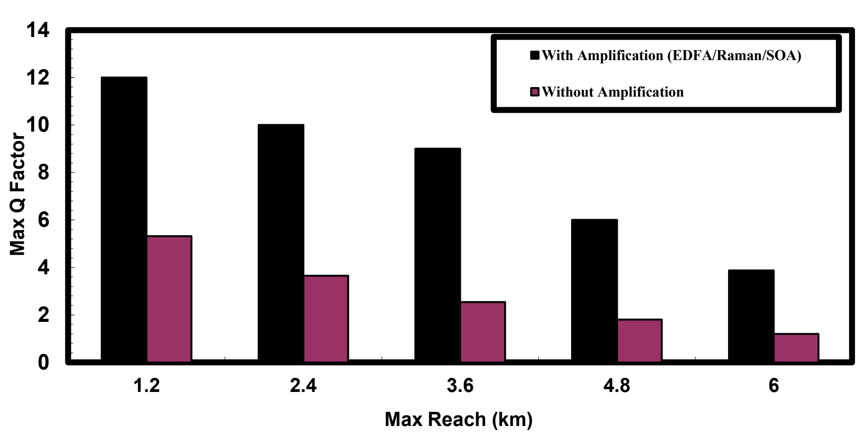

Figure 12: Max. *Q* factor variations versus max reach variations after PIN photodetector receiver under light rain weather conditions at 40 Gbps with/ without amplification units.

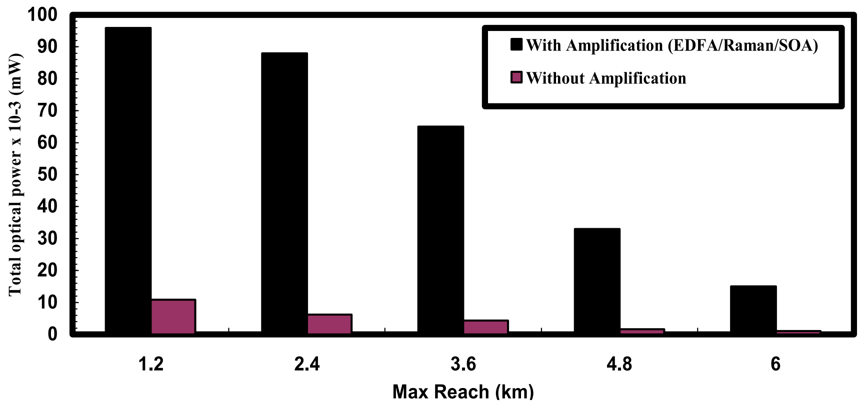

Figure 13: Total optical power variations versus max reach variations after FSO channel under light rain weather conditions at 10 Gbps with/without amplification units.

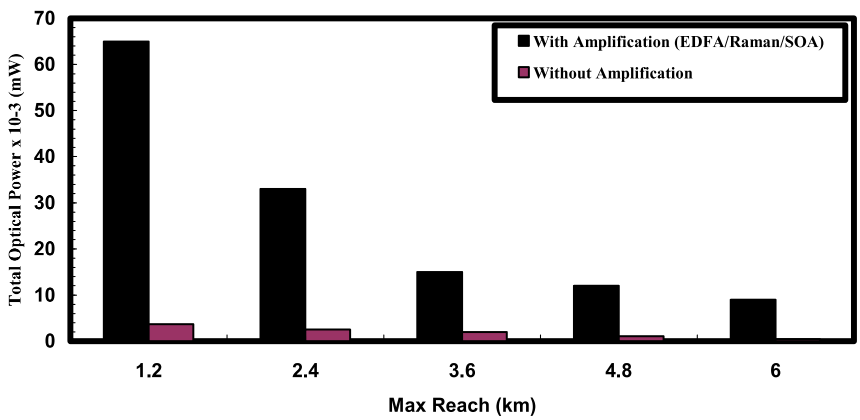

Figure 14: Total optical power variations versus max reach variations after FSO channel under light rain weather conditions at 40 Gbps with/without amplification units.

light rain weather conditions at 10 Gbps with/without amplification units. The total optical power is 95.87 μW with the amplification unit, 10.9 μW without the amplification unit at reach of 1.2 km. As well as the total optical power is 88 μW with the amplification unit, 6.2 μW without the amplification unit at reach of 2.4 km. Also the total optical power is 65 μW with the amplification unit, 4.3 μW without the amplification unit at reach of 3.6 km. Besides the total optical power is 33 μW with the amplification unit, 1.6 μW without the amplification unit at reach of 4.8 km. Moreover the total optical power is 15 μW with the amplification unit, 1 μW without the amplification unit at reach of 6 km.

Figure 14 assures the total optical power variations versus max reach variations after FSO channel under light rain weather conditions at 40 Gbps with/without amplification units. The total optical power is 65 μW with the amplification unit, 3.65 μW without the amplification unit at reach of 1.2 km. As well as the total optical power is 33 μW with the amplification unit, 2.54 μW without the amplification unit at reach of 2.4 km. Also the total optical power is 15 μW with the amplification unit, 1.987 μW without the amplification unit at reach of 3.6 km. Besides the total optical power is 12 μW with the amplification unit, 1.1 μW without the amplification unit at reach of 4.8 km. Moreover the total optical power is 9 μW with the amplification unit, 0.5 μW without the amplification unit at reach of 6 km.

4 Conclusions

We have deeply simulated performance efficiency of carrier suppressed non return to zero line coding based FSO transceiver systems under light rain conditions with/without amplification units. The obtained results assured that the higher the FSO channel reach the lower the total optical power and *Q* factor in the FSO transceiver system. The amplification unit has presented better performance in FSO channel reach and max *Q* factor can be enhanced. The FSO transceiver is tested to measure total optical power, max *Q* and min BER in the system with 10 and 40 Gbps. The study emphasized that the obtained FSO Reach is 6 km with amplification unit and 1.2 km without amplification unit under light rain weather conditions.

Author contributions: All the authors have accepted responsibility for the entire content of this submitted manuscript and approved submission.
Research funding: None declared.
Conflict of interest statement: The authors declare no conflicts of interest regarding this article.

References

1. Lee JH, Chung TM. Secure handover for proxy mobile IPv6 in next-generation communications: scenarios and performance. Wirel Commun Mob Comput J 2011;11:176–86.
2. Sarkar S, Dixit S, Mukherjee B. Hybrid wireless optical broadband access network (WOBAN): a review of relevant challenges. IEEE/OSA J Light Technol 2007;25:1233–9.
3. Rashed ANZ, Mohamed AENA, Sharshar HA, Salah Tabour M, El-Sherbeny A. Optical cross connect performance enhancement in optical ring metro network for extended number of users and different bit rates employment. Wirel Pers Commun Journal 2017;94:927–47.
4. Rashed ANZ, Gawad Mohamed AENAE, Salman Hanafy SAER, Aly MH. A comparative study of the performance of graded index perfluorinated plastic and alumino silicate optical fibers in internal optical interconnections. Optik J 2016;127:9259–63.
5. Rashed ANZ, Tabour MSF, El-Meadawy S. Optimum flat gain with optical amplification technique based on both gain flattening filters and fiber bragg grating methods. J Nanoelectron Optoelectron 2018;13:665–76.
6. Rashed ANZ, Tabbour MSF. Suitable optical fiber communication channel for optical nonlinearity signal processing in high optical data rate systems. Wirel Pers Commun J 2017;97:397–416.
7. Rashed ANZ, Tabbour MSF. The trade-off between different modulation schemes for maximum long reach high data transmission capacity optical orthogonal frequency division multiplexing (OOFDM). Wirel Pers Commun J 2018;101:325–37.
8. Rashed ANZ, Abdel Kader HM, Al-Awamry AA, Abd El-Aziz IA. Transmission performance simulation study evaluation for high speed radio over fiber communication systems. Wirel Pers Commun J 2018;103:1765–79.
9. Rashed ANZ, Tabbour MSF. Best candidate integrated technology for low noise, high speed, and wide bandwidth based transimpedance amplifiers in optical computing systems and optical fiber applications. Int J Commun Syst 2018;31: e3801.
10. Rashed ANZ, Tabbour MSF, El-Assar M. 20 Gb/s hybrid CWDM/DWDM for extended reach fiber to the home network applications. Proc Natl Acad Sci India Sect A Phys Sci 2019;89: 653–62.
11. Hennier H, Wilfert O. An introduction to free space optical communications. Radio Eng J 2010;19:203–12.
12. Peng M, Wang W, Zhang J. Investigation of capacity and call admission control schemes in TD-SCDMA uplink systems employing smart antenna techniques. Wirel Commun Mob Comput 2010;10:241–56.
13. Boopathi CS, Vinoth Kumar K, Sheebarani S, Selvakumar K, Rashed ANZ, Yupapin P. Design of human blood sensor using symmetric dual core photonic crystal fiber. Results Phys 2018; 11:964–5.
14. Vigneswaran D, Mani Rajan MS, Aly MH, Rashed ANZ. Few-mode ring core fiber characteristics: temperature impact. Photonic Netw Commun 2018;15:34–43.
15. Praveen Chakkravarthy S, Arthi V, Karthikumar S, Rashed ANZ, Yupapin P, Amiri IS. Ultra high transmission capacity based on optical first order soliton propagation systems. Results Phys 2019;12:512–3.
16. Rashed ANZ, Vinoth Kumar K, Prithi S, Maheswar R, Tabbour MSF. Transmittivity/reflectivity, bandwidth, and ripple factor level measurement for different refractive index fiber grating shape profiles. J Opt Commun 2019;1–12. https://doi.org/10.1515/joc-2018-0233.
17. Zaki Rashed AN, Vinoth Kumar K, Venkatesh Kumar P, Mohamed AENA, Tabbour MS, El-Assar M. DWDM channel spacing effects on the signal quality for DWDM/CWDM FTTx network. J Opt Commun 2019;1–9. https://doi.org/10.1515/joc-2019-0012.
18. Zaki Rashed AN, Tabbour MSF, Vijayakumari P. Numerical analysis of optical properties using octagonal shaped photonic crystal fiber. J Opt Commun 2019;1–8. https://doi.org/10.1515/joc-2019-0013.
19. Zaki Rashed AN, Satheesh Kumar S, Tabbour MSF, Sundararajan TVP, Maheswar R. Different graded refractive index fiber profiles design for the control of losses and dispersion effects. J Opt Commun 2019;1–6. https://doi.org/10.1515/joc-2019-0036.
20. Majumdar AK, Ricklin JC. Free space laser communications, principles and advantages. California: Springer Science; 2008.
21. Juarez JC, Dwivedi A, Hammons AR, Jones SD, Weerackody V, Nichols RA. Free space optical communications for next generation military networks. IEEE Commun Mag 2006;2:46–51.
22. Zaki Rashed AN. Comparison between NRZ/RZ modulation techniques for upgrading long haul optical wireless communication systems. J Opt Commun 2019;1–7. https://doi.org/10.1515/joc-2019-0038.
23. Zaki Rashed AN, Vinoth Kumar K, Tabbour MSF, Sundararajan TVP. Nonlinear characteristics of semiconductor optical amplifiers for optical switching control realization of logic gates. J Opt Commun 2019;1–6. https://doi.org/10.1515/joc-2019-0027.
24. Ahmed K, Kumar Paula B, Vasudevan B, Zaki Rashed AN, Maheswar R, Amiri IS, et al. Design of D-shaped elliptical core photonic crystal fiber for blood plasma cell sensing application. Results Phys 2019;12:2021–5.
25. Ramana TV, Pandian A, Ellammal C, Jarin T, Zaki Rashed AN, Sampathkumar A. Numerical analysis of circularly polarized modes in coreless photonic crystal fiber. Results Phys 2019;13: 102140.
26. Zaki Rashed AN, Mohammed AENA, Fawzy Zaky W, Amiri IS, Yupapin P. The switching of optoelectronics to full optical computing operations based on nonlinear metamaterials. Results Phys 2019;13:102152.
27. Ranathive S, Vinoth Kumar K, Zaki Rashed AN, Tabbour MSF, Sundararajan TVP. Performance signature of optical fiber communications dispersion compensation techniques for the control of dispersion management. J Opt Commun 2019;1–8. https://doi.org/10.1515/joc-2019-0021.

28. Giggenbach D, Horwath J, Epple B. Optical satellite downlinks to optical ground stations and high-altitude platforms. Budapest, Hungary: IST Mobile & Wireless Communication Summit; 2007.
29. Aliba M, Oawa K, Ito S. Measurement and simulation of the effect of snow fall on free space optical propagation. Appl Opt 2008; 47:5736–43.
30. Amiri IS, Zaki Rashed AN, Yupapin P. Interaction between optical sources and optical modulators for high-speed optical communication networks. J Opt Commun 2019;1–7. https://doi.org/10.1515/joc-2019-0041.
31. Amiri IS, Zaki Rashed AN, Yupapin P. Effects of order super Gaussian pulses on the performance of high data rate optical fiber channel in the presence of self-phase modulation. J Opt Commun 2019;1–5. https://doi.org/10.1515/joc-2019-0039.
32. Amiri IS, Zaki Rashed AN, Yupapin P. Mathematical model analysis of dispersion and loss in photonic crystal fibers. J Opt Commun 2019;1–7. https://doi.org/10.1515/joc-2019-0052.
33. Amiri IS, Zaki Rashed AN, Yupapin P. Basic functions of fiber bragg grating effects on the optical fiber systems performance efficiency. J Opt Commun 2019;1–13. https://doi.org/10.1515/joc-2019-0042.
34. Amiri IS, Zaki Rashed AN, Mohammed AENA, Aboelazm MB, Yupapin P. Nonlinear effects with semiconductor optical amplifiers. J Opt Commun 2019;1–17. https://doi.org/10.1515/joc-2019-0053.
35. Amiri IS, Zaki Rashed AN, Yupapin P. High-speed light sources in high-speed optical passive local area communication networks. J Opt Commun 2019;1–12. https://doi.org/10.1515/joc-2019-0070.
36. Zaki Rashed AN, Tabbour MSF, Natarajan K. Performance enhancement of overall LEO/MEO intersatellite optical wireless communication systems. Int J Satell Commun Netw 2020;38: 31–40.
37. Bielecki Z, Kolosowski W, Mikolajczyk J. Free space optical data link using quantum cascade laser. In: PIERS proceedings. Cambridge, USA; 2008.
38. Andre PS, Pinto AN, Pinto JL, Almeida T, Pousa M. Selective wavelength transparent optical add-drop multiplexer based on fiber bragg gratings. J Opt Commun 2006;24:222–9.
39. Amiri IS, Zaki Rashed AN, Mohammed AEA, El-Din ES, Yupapin P. Spatial continuous wave laser and spatiotemporal VCSEL for high-speed long haul optical wireless communication channels. J Opt Commun 2019;1–16. https://doi.org/10.1515/joc-2019-0061.
40. Amiri IS, Mahmoud Houssien FMA, Zaki Rashed AN, Mohammed AENA. comparative simulation of thermal noise effects for photodetectors on performance of long-haul DWDM optical networks. J Opt Commun 2019;1–9. https://doi.org/10.1515/joc-2019-0152.
41. Amiri IS, Zaki Rashed AN, Yupapin P. Average power model of optical Raman amplifiers based on frequency spacing and amplifier section stage optimization. J Opt Commun 2019;1–10. https://doi.org/10.1515/joc-2019-0081.
42. Amiri IS, Mahmoud Houssien FMA, Zaki Rashed AN, Mohammed AENA. Temperature effects on characteristics and performance of near-infrared wide bandwidth for different avalanche photodiodes structures. Results Phys 2019;14: 102399.
43. Amiri IS, Zaki Rashed AN. Simulative study of simple ring resonator-based Brewster plate for power system operation stability. Indones J Electr Eng Comput Sci 2019;16:1070–6.
44. Amiri IS, Zaki Rashed AN. Different photonic crystal fibers configurations with the key solutions for the optimization of data rates transmission. J Opt Commun 2019;1–11. https://doi.org/10.1515/joc-2019-0100.
45. Amiri IS, Zaki Rashed AN, Ramya KC, Vinoth Kumar K, Maheswar R. The physical parameters of EDFA and SOA optical amplifiers and bit sequence variations based optical pulse generators impact on the performance of soliton transmission systems. J Opt Commun 2019;1–8. https://doi.org/10.1515/joc-2019-0156.
46. Amiri IS, Mahmoud Houssien FMA, Zaki Rashed AN, Mohammed AENA. Optical networks performance optimization based on hybrid configurations of optical fiber amplifiers and optical receivers. J Opt Commun 2019;1–8. https://doi.org/10.1515/joc-2019-0153.
47. Amiri IS, Zaki Rashed AN, Sarker K, Paul BK, Ahmed K. Chirped large mode area photonic crystal modal fibers and its resonance modes based on finite element technique. J Opt Commun 2019; 1–15. https://doi.org/10.1515/joc-2019-0146.
48. Alnajjar SH, Ali MH, Al-Obaidi A, Alsaedi MA. Hybrid of multiple (TX/RX) FSO/fiber optic communication system under environmental disturbances. J Multidiscip Res 2020;2:7–16.
49. Yu YL, Liaw SK, Chou HH, Le-Minh H, Ghassemlooy Z. A hybrid optical fiber and FSO system for bidirectional communications used in bridges. IEEE Photonics J 2015;7:1–9.
50. Zaki Rashed AN, Tabbour MSF, El-Meadawy S, Anwar T, Sarlan A, Yupapin P, et al. The effect of using different materials on erbium-doped fiber amplifiers for indoor applications. Results Phys 2019;15:102650.
51. Amiri IS, Zaki Rashed AN. Power enhancement of the U-shape cavity microring resonator through gap and material characterizations. J Opt Commun 2019;1–14. https://doi.org/10.1515/joc-2019-0108.
52. Amiri IS, Kuppusamy PG, Zaki Rashed AN, Jayarajan P, Thiyagupriyadharsan MR, Yupapin P. The engagement of hybrid ultra-high space division multiplexing with maximum time division multiplexing techniques for high-speed single-mode fiber cable systems. J Opt Commun 2019;1–13. https://doi.org/10.1515/joc-2019-0205.
53. Amiri IS, Zaki Rashed AN, Jahan S, Paul BK, Ahmed K. Polar polarization mode and average radical flux intensity measurements based on all optical spatial communication systems. J Opt Commun 2019;1–18. https://doi.org/10.1515/joc-2019-0159.
54. Sivaranjani S, Sampathkumar A, Zaki Rashed AN, Sundararajan TVP, Amiri IS. Performance evaluation of bidirectional wavelength division multiple access broadband optical passive elastic networks operation efficiency. J Opt Commun 2019;1–20. https://doi.org/10.1515/joc-2019-0175.
55. Amiri IS, Zaki Rashed AN, Yupapin P. High-speed transmission circuits signaling in optical communication systems. J Opt Commun 2019;1–19. https://doi.org/10.1515/joc-2019-0197.
56. Alatwi AM, Zaki Rashed AN, El-Gammal EM. Wavelength division multiplexing techniques based on multi transceiver in low earth orbit intersatellite systems. J Opt Commun 2020;1–9. https://doi.org/10.1515/joc-2019-0171.

57. El-Hageen HM, Kuppusamy PG, Alatwi AM, Sivaram M, Yasar ZA, Zaki Rashed AN. Different modulation schemes for direct and external modulators based on various laser sources. J Opt Commun 2020;1–8. https://doi.org/10.1515/joc-2020-0029.
58. El-Hageen HM, Alatwi AM, Zaki Rashed AN. High-speed signal processing and wide band optical semiconductor amplifier in the optical communication systems. J Opt Commun 2020;1–6. https://doi.org/10.1515/joc-2020-0070.
59. El-Hageen HM, Alatwi AM, Zaki Rashed AN. Laser measured rate equations with various transmission coders for optimum of data transmission error rates. Indones J Electr Eng Comput Sci 2020; 20:1406–12.
60. Eid MMA, Ahasan Habib M, Shamim Anower M, Zaki Rashed AN. Highly sensitive nonlinear photonic crystal fiber based sensor for chemical sensing applications. Microsyst Technol 2020;28: 134–45. https://doi.org/10.1007/s00542-020-05019-w.
61. Eid MMA, Zaki Rashed AN, Shafkat A, Ahmed K. Fabry Perot laser properties with high pump lasers for upgrading fiber optic transceiver systems. J Opt Commun 2020;1–13. https://doi.org/10.1515/joc-2020-0146.
62. Eid MMA, Zaki Rashed AN, Sazib Hosen M, Paul BK, Ahmed K. Spatial optical transceiver system–based key solution for high data rates in measured index multimode optical fibers for indoor applications. J Opt Commun 2020;1–14. https://doi.org/10.1515/joc-2020-0117.
63. Eid MMA, Zaki Rashed AN, El-Meadawy S, Ahmed K. Simulation study of signal gain optimization based on hybrid composition techniques for high speed optically dense multiplexed systems. J Opt Commun 2020;1–16. https://doi.org/10.1515/joc-2020-0150.
64. Alatwi AM, Zaki Rashed AN. Hybrid CPFSK/OQPSK modulation transmission techniques' performance efficiency with RZ line coding–based fiber systems in passive optical networks. Indones J Electr Eng Comput Sci 2021;21:263–270.
65. Alatwi AM, Zaki Rashed AN. An analytical method with numerical results to be used in the design of optical slab waveguides for optical communication system applications. Indones J Electr Eng Comput Sci 2021;21:278–86.
66. Alatwi AM, Zaki Rashed AN. Conventional doped silica/fluoride glass fibers for low loss and minimum dispersion effects. Indones J Electr Eng Comput Sci 2021;21:287–95.
67. El-Hageen HM, Alatwi AM, Zaki Rashed AN. Spatial optical transmitter based on on/off keying line coding modulation scheme for optimum performance of telecommunication systems. Indones J Electr Eng Comput Sci 2021;21:305–12.
68. Eid MMA, Rashed ANZ, Kurmendra. High speed optical switching gain based EDFA model with 30 Gb/s NRZ modulation code in optical systems. J Opt Commun 2020;1–15. https://doi.org/10.1515/joc-2020-0223.
69. Eid MMA, Amiri IS. Fast speed switching response and high modulation signal processing bandwidth through LiNbO3 electro-optic modulators. J Opt Commun 2020;1–14. https://doi.org/10.1515/joc-2020-0012.
70. Eid MMA, Mahmoud Houssien FMA, Zaki Rashed AN, Mohammed AENA. Performance enhancement of transceiver system based inter satellite optical wireless channel (IS-OWC) for ultra-long distances. J Opt Commun 2020;1–18. https://doi.org/10.1515/joc-2020-0216.
71. El-din ES. Simulation performance signature evolution of optical inter satellite links based booster EDFA and receiver preamplifiers. J Opt Commun 2020;1–19. https://doi.org/10.1515/joc-2020-0190.
72. El-gammal EM. Influence of dense wavelength division multiplexing (DWDM) technique on the low earth orbit intersatellite systems performance. J Opt Commun 2020;1–12. https://doi.org/10.1515/joc-2020-0188.
73. Eid MMA, Al-Mamun Bulbul A, Podder E. Mono rectangular core photonic crystal fiber (MRC-PCF) for skin and blood cancer detection. Plasmonics J 2020;34:654–60.
74. Eid MMA, Seliem AS, Zaki Rashed AN, Mohammed AENA, Ali MY, Abaza SS. High speed pulse generators with electro-optic modulators based on different bit sequence for the digital fiber optic communication links. Indones J Electr Eng Comput Sci 2021;21:957–67.
75. Eid MMA, Seliem AS, Zaki Rashed AN, Mohammed AENA, Ali MY, Abaza SS. The key management of direct/external modulation semiconductor laser response systems for relative intensity noise control. Indones J Electr Eng Comput Sci 2021; 21:968–77.
76. Habib A, Zaki Rashed AN, El-Hageen HM, Alatwi AM. Extremely sensitive photonic crystal fiber–based cancer cell detector in the terahertz regime. Plasmonics 2020;43:1243–55.
77. Shafkat A, Zaki Rashed AN, El-Hageen HM, Alatwi AM. Design and analysis of a single elliptical channel photonic crystal fiber sensor for potential malaria detection. J Sol Gel Sci Technol 2020;38:655–66.
78. Eid MMA, Zaki Rashed AN. Fixed scattering section length with variable scattering section dispersion based optical fibers for polarization mode dispersion penalties. Indones J Electr Eng Comput Sci 2021;21:1540–7.
79. Eid MMA, Seliem AS, Zaki Rashed AN, Mohammed AENA, Ali MY, Abaza SS. High sensitivity sapphire FBG temperature sensors for the signal processing of data communications technology. Indones J Electr Eng Comput Sci 2021;21:1567–74.
80. Eid MMA, Seliem AS, Zaki Rashed AN, Mohammed AENA, Ali MY, Abaza SS. High modulated soliton power propagation interaction with optical fiber and optical wireless communication channels. Indones J Electr Eng Comput Sci 2021; 21:1575–83.
81. Singh M, Malhotra J. 40 Gbit/s-80 GHz hybrid MDM-OFDM-Multibeam based RoFSO transmission link under the effect of adverse weather conditions with enhanced detection. Optoelectron Adv Mater Rapid Commun 2019;14:146–53.
82. Singh M, Malhotra J. 4×20 Gbit/s-40 GHz OFDM based Radio over FSO transmission link incorporating hybrid wavelength division multiplexing-mode division multiplexing of LG and HG modes with enhanced detection. Optoelectron Adv Mater Rapid Commun 2020;14:233–43.
83. Zaki Rashed AN. High reliability optical interconnections for short range applications in high speed optical communication systems. Opt Laser Technol 2013;48:302–8.
84. Zaki Rashed AN. High performance photonic devices for multiplexing/demultiplexing applications in multi band operating regions. J Comput Theor Nanosci 2012;9:522–31.
85. Zaki Rashed AN. Optical fiber communication cables systems performance under harmful gamma irradiation and thermal environment effects. IET Commun 2013;7:448–55.
86. Zaki Rashed AN. Performance signature and optical signal processing of high speed electro-optic modulators. Opt Commun 2013;294:49–58.

87. Zaki Rashed AN. High efficiency wireless optical links in high transmission speed wireless optical communication networks. Int J Commun Syst 2014;27:3416–27.
88. Zaki Rashed AN. High efficiency laser power transmission with all optical amplification for high transmission capacity submarine cables. J Russ Laser Res 2013;34:603–13.
89. Zaki Rashed AN. Submarine fiber cable network systems cost planning considerations with achieved high transmission capacity and signal quality enhancement. Opt Commun 2014; 311:44–54.
90. Al-Khaffaf DAJ, Alsahlany AM. A cloud VLC access point design for 5G and beyond. Opt Quant Electron 2021;53:472–81.
91. Al-Khaffaf DAJ, Alsahlany AM. 60 GHz millimetre wave/10 Gbps transmission for super broadband Wi-Fi network. J Commun 2019;14:261–6.
92. Al-Khaffaf DAJ, Rashid Hujijo HS. High data rate optical wireless communication system using millimeter wave and optical phase modulation. ARPN J Eng Appl Sci 2018;13:9086–92.
93. Al-Khaffaf DAJ, Alshimaysawe IA. Miniaturised tri-band microstrip patch antenna design for radio and millimetre waves of 5G devices. Indones J Electr Eng Comput Sci 2021;21:594–601.
94. Bloom S, Korevaar E, Schuster J, Willebrand H. Understanding the performance of free-space optics. J Opt Netw 2003;2: 178–200.
95. Eid MMA, Mohammed AENA, Zaki Rashed AN. Different soliton pulse order effects on the fiber communication systems performance evaluation. Indones J Electr Eng Comput Sci 2021; 23:1485–92.
96. Urooj S, Muhammad Alwadai N, Sorathiya V, Lavadiya S, Parmar J, Patel SK, et al. Differential coding scheme based FSO channel for optical coherent DP-16 QAM transceiver systems. J Opt Commun 2021;1–12. https://doi.org/10.1515/joc-2021-0118.
97. Zaki Rashed AN, Fawzy Zaky W, Eid MMA, Faragallah OS. Dynamic response based on non-linear material for electrical and optical analogy of full optical oscillator. Opt Quant Electron 2021;53:658.
98. Zaki Rashed AN, Fawzy Zaky W, El-Hageen HM, Alatwi AM. Technical specifications for an all-optical switch for information storage and processing systems. Eur Phys J Plus 2021;136:1100. https://doi.org/10.1140/epjp/s13360-021-01841-x.
99. Sorathiya V, Lavadiya S, Parmar B, Das S, Krishna M, Faragallah OS, et al. Numerical investigation of the tunable polarizer using gold array and graphene metamaterial structure for an infrared frequency range. Appl Phys B 2022;128:13.
100. Delwar TS, Siddique A, Biswal MR, Behera P, Zaki Rashed AN, Choi Y, et al. A novel dual mode configurable and tunable high-gain, high-efficient CMOS power amplifier for 5G applications. Integrat VLSI J 2022;83:77–87.
101. Eid MMA, Arunachalam R, Sorathiya V, Lavadiya S, Patel SK, Parmar J, et al. QAM receiver based on light amplifiers measured with effective role of optical coherent duobinary transmitter. J Opt Commun 2022;1–16. https://doi.org/10.1515/joc-2021-0205.
102. Sorathiya V, Lavadiya S, Ahmed AG, Faragallah OS, El-Sayed HS, Parmar B, et al. Hilbert resonator based multiband tunable graphene metasurface polarizer for lower THz frequency. J Comput Electron 2022;44:333–40.
103. Mohammad A, Alzaidi MS, Eid MMA, Sorathiya V, Lavadiya S, Patel SK, et al. First order surface grating fiber coupler under the period chirp and apodization functions variations effects. Indones J Electr Eng Comput Sci 2022;25:1020–9.
104. Mohammad A, Alzaidi MS, Eid MMA, Sorathiya V, Lavadiya S, Patel SK, et al. Free space optical communication system for indoor applications based on printed circuit board design. Indones J Electr Eng Comput Sci 2022;25:1030–7.
105. Sorathiya V, Lavadiya S, Singh Parmar B, Baxi S, Taher Dhankot, Faragallah OS, et al. Tunable squared patch based graphene metasurface infrared polarizer. Appl Phys B 2022;45:1230–42.
106. Lavadiya S, Sorathiya V, Faragallah OS, El-Sayed HS, Eid MMA, Zaki Rashed AN. Infrared graphene assisted multi-band tunable absorber. Opt Quant Electron 2022;54:134.
107. Habib Jibon R, Ahmed M, Abd-Elnaby M, Zaki Rashed AN, Eid MMA. Design mechanism and performance evaluation of photonic crystal fiber (PCF) based sensor in the THz regime for sensing noxious chemical substrates of poultry feed. Appl Phys A 2022;128:169.
108. Sorathiya V, Lavadiya S, Thomas L, Abd-Elnaby M, Zaki Rashed AN, Eid MMA. Graphene based tunable short band absorber for infrared wavelength. Appl Phys B 2022;128:40.
109. Dutta N, Patel SK, Faragallah OS, Baz M, Zaki Rashed AN. Caching scheme for information-centric networks with balanced content distribution. Int J Commun Syst 2022;54:e5104. https://doi.org/10.1002/dac.5104.
110. Lavadiya SP, Sorathiya V, Kanzariya S, Chavda B, Naweed A, Faragallah OS, et al. Low profile multiband microstrip patch antenna with frequency reconfigurable feature using PIN diode for S, C, X, and Ku band applications. Int J Commun Syst 2022;55: e5141.
111. Asaduzzaman S, Rehana H, Aziz T, Faragallah OS, Baz M, Eid MMA, et al. Key performance parameters estimation with Epsilon near zero (ENZ) for Kagome photonic crystal fiber in THz system. Opt Quant Electron 2022;54:202.
112. Patel SK, Solanki N, Charola S, Parmar J, Zakaria R, Faragallah OS, et al. Graphene based highly sensitive refractive index sensor using double split ring resonator metasurface. Opt Quant Electron 2022;54:203.
113. Sorathiya V, Lavadiya S, Faragallah OS, Eid MMA, Zaki Rashed AN. D shaped dual core photonics crystal based refractive index sensor using graphene–titanium–silver materials for infrared frequency spectrum. Opt Quant Electron 2022;54:290.
114. Hossain E, Shazzad Hossain M, Selim Hossain M, Al Jannat S, Huda M, Alsharif S, et al. Brain tumor auto-segmentation on multimodal imaging modalities using deep neural network. Comput Mater Continua 2022;72:4509–23.
115. Asaduzzaman S, Rehana H, Rana C, Faragallah OS, El-Sayed HS, Eid MMA, et al. Hexa sectored square photonic crystal fiber for blood serum and plasma sensing with ultralow confinement loss. Appl Phys A 2022;128:467.
116. Omollo Nyangaresi V, Abd-Elnaby M, Eid MMA, Zaki Rashed AN. Trusted authority based session key agreement and authentication algorithm for smart grid networks. Trans Emerg Telecommun Technol 2022:1e4528–16. https://doi.org/10.1002/ett.4528.
117. Sunitha G, Arunachalam R, Abd-Elnaby M, Eid MMA, Zaki Rashed AN. A comparative analysis of deep neural network on acoustic cough features. Int J Imag Syst Technol 2022;35:1–14.
118. Sorathiya V, Faragallah OS, El-Sayed HS, Eid MMA, Zaki Rashed AN. Nanofocusing of optical wave using staircase tapered plasmonic waveguide. Appl Phys B 2022;128:104.